JTCM Journal of Traditional Chinese Medicine

Online Submissions: http://www.journaltcm.com
ISSN 0255-2922
info@journaltcm.com

Research Article

Acupotomy inhibits aberrant formation of subchondral bone through regulating osteoprotegerin/receptor activator of nuclear factor-κB ligand pathway in rabbits with knee osteoarthritis induced by modified Videman method

QIN Luxue, GUO Changqing, ZHAO Ruili, WANG Tong, WANG Junmei, GUO Yan, ZHANG Wei, HU Tingyao, CHEN Xilin, ZHANG Qian, ZHANG Dian, XU Yue

QIN Luxue, GUO Changqing, WANG Tong, WANG Junmei, HU Tingyao, CHEN Xilin, ZHANG Qian, ZHANG Dian, XU Yue, School of Acupuncture-Moxibustion and Tuina, Beijing University of Chinese Medicine, Beijing 100029, China
ZHAO Ruili, the First People's Hospital of Dongcheng District, Beijing 100050, China
GUO Yan, Beijing Hospital of Traditional Chinese Medicine, Capital Medical University, Beijing 100010, China.
ZHANG Wei, the Third Affiliated Hospital of Beijing Universality of Chinese Medicine, Beijing 100029, China
Supported by the Beijing Municipal Natural Science Foundation: To Explore the Effect of Acupotomy on Subchondral Bone Remodeling in Early and Middle KOA Based on OPG/RANKL/RANK pathway (7192110)
Correspondence to: Prof. GUO Changqing, School of Acupuncture-Moxibustion and Tuina, Beijing University of Chinese Medicine, Beijing 100029, China. Guochangqing66@163.com
Telephone: +86-10-64286687
DOI: 10.19852/j.cnki.jtcm.2022.03.006
Received: October 22, 2021
Accepted: December 1, 2022
Available online: May 20, 2022

Abstract

OBJECTIVE: To investigate the effects of acupotomy on inhibiting abnormal formation of subchondral bone in rabbits with knee osteoarthritis (KOA).

METHODS: A total of 24 New Zealand rabbits were randomly divided into four groups of 6 rabbits each [control, model, electroacupuncture (EA) and acupotomy]. Eighteen KOA model rabbits were established using a modified Videman method. Rabbits in EA and acupotomy groups received the intervention for 3 weeks. Then, the cartilage and subchondral bone unit were obtained and the histomorphological changes were recorded. Osteoprotegerin (OPG) and receptor activator of nuclear factor-κB ligand (RANKL) in subchondral bone were evaluated by Western blotting, real-time polymerase chain reaction and immunohistochemistry.

RESULTS: Compared with the model group, both the acupotomy and EA groups showed a significant decrease in the Lequesne index (both $P < 0.01$) and Mankin score ($P < 0.01$, < 0.05). In addition, both EA and acupotomy groups had a higher expression of total articular cartilage (TAC) ($P < 0.05$, < 0.01) and lower expression of articular calcified cartilage (ACC)/TAC ($P < 0.05$, < 0.05) compared with the model group. The thickness of the subchondral bone plate in EA and acupotomy groups were decreased (both $P < 0.01$) compared to the model group. Moreover, trabecular bone volume (BV/TV), protein and relative expression of OPG and the ratio of OPG/RANKL in the subchondral bone of acupotomy group were decreased statistically significant, while these parameters were not significantly changed in the EA group compared with the model group.

CONCLUSIONS: In the rabbit model of KOA, acupotomy inhibits aberrant formation of subchondral bone by suppressing OPG/RANKL ratio as a potential therapy for KOA.

Keywords: acupuncture therapy; osteogenesis; osteoarthritis, knee; subchondral bone

1. INTRODUCTION

Osteoarthritis (OA) is a chronic disease of joints, which is manifested as cartilage degeneration, and will result in progressive pain, function loss and frequent disability. Knee osteoarthritis (KOA) is prevalent in people aged 50 years old or older, affecting more than 250 million patients worldwide.[1] At an advanced stage of KOA, total joint replacement surgery brings remarkable pain relief and substantial functional improvement.[2] However, considering surgical risks and economic costs, it is critical to develop new complementary therapeutic strategies.

KOA is characterized by cartilage degeneration, synovium inflammation, osteophytes, subchondral bone sclerosis and osteophyte formation.[3] In recent years, studies have found that subchondral bone remodeling

may occur earlier than cartilage destruction.[4] Mechanical overloading results in ultrastructural damage of the subchondral bone, especially to collagen fiber, which in turn destroys the integrity of the subchondral bone, increases the load of covering cartilage, and ultimately leads to cartilage damage and degradation.[5]

During the normal process of bone remodeling, the resorption and osteoblast-mediated formation of bone is maintained as a delicate balance.[6] During the early stages of KOA, abnormal mechanical loading induces subchondral bone microcracks, and leads to its remodeling.[7] Thus, the direct results of bone remodeling are osteoporosis, thinning of trabeculae and reduction of plate thickness. During the late stage of KOA, microfracture healing process favors bone formation, which might result in subchondral bone sclerosis and thickening.[8]

Fundamentally, continuous remodeling of bone tissue could be achieved by interactions between osteoblasts and osteoclasts.[9] The molecular osteoprotegerin (OPG)/receptor activator of nuclear factor-κB ligand (RANKL)/RANK system is known for its role in osteoclasts maturation and bone remodeling. OPG and RANKL are mainly secreted by osteoblasts, while RANK is expressed at the surface of osteoclasts. RANK acts to cause osteoclast proliferation and differentiation through the interaction with RANKL, which contributes to bone resorption. Whereas OPG acts as a decoy receptor of RANKL to inhibit bone resorption by blocking the binding of RANK to RANKL.[10] Therefore, OPG/RANKL ratio is an important indicator reflecting the activity level of osteoclasts.[11] The ratio of RANKL/OPG in KOA showed a trend of rising first and then followed by falling, which was consistent with the pathological changes of bone resorption in early stage and bone formation in late stage.[12]

It is widely believed that mechanical imbalance plays an important role in the pathogenesis of KOA. Treatments which correct the abnormal stress have long lasting beneficial effects on pain and function compared with steroids and nonsteroidal anti-inflammatory drugs, which have just transient effects.[13] Acupotomy therapy is a biomechanical intervention based on modern anatomy and guided by the theory of Traditional Chinese Medicine, which has shown therapeutic promise in clinical trials for KOA by releasing soft tissues and correcting abnormal mechanics. Previous studies have found that both acupotomy and Electroacupuncture (EA) effectively improved the clinical symptoms by inhibiting the inflammatory factors such as TNF-α, IL-6 and IL-1β.[14] and increased in the matrix anabolism of articular cartilage via up-regulations of collagen II and aggrecan expression and down-regulation of MMP3 expression through activating the integrinβ1 signaling pathway in KOA rabbits.[15,16] Acupotomy achieved relatively better efficacy than the EA. However, little was known about the effect of acupotomy on subchondral bone remodeling. Thus hematoxylin-eosin (HE) staining, scanning electron microscopy, Western blotting (WB), quan- titative real-time (QRT)-PCR, and immune-ohistochemical analyses were used in this study to explore the effect of acupotomy and EA on the formation of subchondral bone in moderate stage of KOA.

2. MATERIALS AND METHODS

2.1. Experimental animals and grouping.

Twenty four 6 months male New Zealand white rabbits (weigh 2.5-3.0 kg, from Keyu Laboratory Animal Technology Co., Ltd., Beijing, China; certificate No. SCXK 2018-0010) were bred in the Institute of Traditional Chinese Medicine, China Academy of Chinese Medical Sciences (CACMS). All animals were raised in separate cages (one cage for each) under controlled temperature (22 ± 2) ℃ and humidity (40%-60%) with standard feeding and watering freely available. The aboratory was disinfected by ultraviolet radiation regularly. The program was approved by the Institute of Traditional Chinese Medicine of CACMS.

The animals were randomly divided into four groups (control, KOA model, EA and acupotomy groups) with 6 rabbits in each. The control group was fed conventionally and all the others were modeled.

2.2. KOA modeling and interventions

The KOA model were established by a modified Videman method.[17] After 10-16h fasting, 3% sodium pentobarbital solution (30 mg/kg) were administered intravenously to each rabbit *via* marginal ear vein under anesthesia. And then the skin of the left hind limb from the groin to the ankle joint was prepared and pulled to make it in a completely straight position. The resin bandage (specification: 15 cm × 360 cm, Suzhou Connect Medical Technology Co., Ltd., soaked in hot water at 65 ℃-85 ℃) was fixed from the groin to the ankle (knee joint extension 180°, ankle dorsal flexion 60°). The toes were exposed for blood supply observation. The bandage was then covered with cotton cloth to prevent rabbits from biting. Motion of animals' left hind limbs was constrained by the bandages for 9 weeks for model preparation. The bandages of all rabbits in each group were removed one week before intervention.

2.3. The control group and the model group: no rabbit underwent any drug treatment or operation

The EA group: disposable sterile acupuncture needles (brand: Huanqiu; diameter: 0.18 mm; length: 13 mm; made by Suzhou Acupuncture and Moxibustion Products Co. LTD) were inserted perpendicularly into the four acupoints: Ququan (LR8), Weiyang (BL39), Neixiyan (EX-LE4) and Waixiyan (ST35). An electroacupuncture apparatus (HANS200A acupoint nerve stimulator, 2 Hz, 3MA) was applied to stimulate the acupoints above for 15 min every 2 d for a period of 3 weeks.

The acupotomy group: the insertion sites included the interfemoral, lateral, rectus and biceps tendon, as well as the joint tendon of sartorius, gracilis and semitendinosus.

After fur carefully trimmed with electric clipper and disinfected with iodophor, the rabbits were performed according to the following procedures: the sharp of the acupotomy needle (HZ series disposable acupotome: 0.35 mm × 25 mm, Maanshan Bond Medical Instruments Co., Ltd.) was parallel to the tendons treated and was inserted vertically into the skin. The experimenter released the tendons in the direction of the bone connection, removed the needle and applied pressure for a moment to stop bleeding. Animals were treated once a week for 3 weeks. All of them were sacrificed one week after the end of treatment. After death, the surrounding soft tissues and ligaments including posterior and anterior cruciate ligament were removed and knee joints were carefully dissected without damaging the cartilage. Cartilage-subchondral bone complex samples were removed from the load-bearing region of the medial tibial plateau (MTP) and lateral tibial plateau (LTP). The sample of LTP was embedded in paraffin for hematoxylin-eosin (HE) staining and immune-ohistochemistry staining. The cartilage on the other samples was shaved off and the rest was divided equally into two parts, one for analysis of real-time PCR and the other for WB. The two parts were placed into liquid nitrogen followed by long storage at −80 ℃.

2.4. Behavioural evaluation

One week after the removal of the bandages and one week after the treatment, all animals were evaluated by the modified Lequesne index scale, which includes four parts: joint pain (0-3 points), joint movement (0-3 points), joint swelling (0-2 points) and gait changes (0-3 points). The assessment was independently completed by two team members (Junmei Wang and Cong Liu). The average score was recorded for data analysis.

2.5. Histology

The cartilage and subchondral bone unit samples were fixed in 4% paraformaldehyde (Coolaber, Beijing, China) for 72 h, decalcified with 10% EDTA for 21 d, embedded in paraffin, and sectioned at 4 μm. The slices were used for haematoxylin and eosin (Zhongkewanbang, Beijing, China) staining and immunohistochemistry (IHC).

The images were visualized by the optical microscope and subsequently analyzed with Image Pro Plus 6.0 software (Media Cybernetics, Silver Spring, MD, USA). Histopathological scoring of cartilage degeneration was done by using the Mankin score. The parameters calculated includes the follows: (a) the distance between the cartilage surface and bonding line (TAC); (b) the distance between the tidemark and bonding line articular calcified cartilage (ACC); (c) TAC/ACC ratio; (d) distance from the bonding line to the interface between the subchondral bone plate and trabecular bone subchondral plate (SBP); (e) trabecular bone volume (BV/TV), which was calculated as follows: (trabecular bone area in the region of measurement)/(trabecular bone area + marrow cavity area) *100.[18] All analyses were carried out by independent examiners who were unaware of the animal identities.

2.6. Immunohistochemistry

For IHC, the paraffin-embedded sections were de-paraffinized with xylene and rehydrated in a graded alcohol series. Sections were washed in xylene, alcohol and PBS respectively, and sections were placed in a repair box filled with EDTA antigen repair buffer (Zhongshanjinqiao, Beijing，China) and antigen repair was conducted at 100 ℃ in the microwave oven for 15 min and then cooled down to room temperature. Next, the samples were incubated with 3% H_2O_2 in PBS during 30 min to block endogenous peroxidases, and incubation was performed with the first antibody (Anti-OPG and anti-RANKL: Bioss, Beijing, China) overnight at 4. At last, DAB was used as the chromogen and hematoxylin was used for counterstained. The number of positively stained cells of RANKL and OPG were counted by Image Pro Plus 6.0 (IPP) image analysis software.

2.7. WB

The samples were removed from liquid nitrogen and placed into a pre-cooled mortar, where they would be pulverized and homogenized rapidly in RIPA buffer. Homogenates were cleared by centrifugation at 1000 r/min for 10 min at 4 ℃, supernatants recovered and the protein concentration quantified with a quantitative bicinchoninic acid (BCA) protein assay. Next, protein samples were separated by 12% sodium dodecyl sulfate-polyacrylamide gel electrophoresis, transferred to Polyvinylidene fluoride (PVDF) membrane, and blocked with 5% skim milk powder by shaking for 60 min at room temperature. Then the membranes were washed 3 × 10 min with Tris Buffered Saline-Tween (TBS-T) and incubated with the appropriate concentration of first antibody in TBS-T overnight at 4 ℃. The next day, the membranes were washed in TBS-T and then incubated with the horseradish peroxidase-conjugated secondary antibody for 60 min at 37 ℃. Finally, the membrane was developed by ECL for visualization of bands and the gray values were analyzed *via* Image-Pro Plus 6.0 software.

The primary and secondary antibodies used in the experiments were anti-OPG (1：100; Novus, CO, USA), anti-RANKL (1：200; Bioss, Beijing, China) and beta actin (1：2000; Zhongshanjinqiao, Beijing, China). Acrylamide, diacrylamide, Lichunhong, sodium dodecyl sulfate, -mercaptoethanol and Protein Molecular Marker were purchased from Bio-rad Co., Ltd., USA. PVDF transfer membranes were purchased from Millipore (Darmstadt, Germany). Photographic films were from Kodak Corporation, New York, USA. Horseradish peroxidase (HRP)-conjugated goat anti-mouse IgG and anti-rabbit IgG were purchased from Zhongshan Golden Bridge Biotechnology Co., Ltd., Beijing, China. The ECL Chemiluminescence kit and BCA protein assay were purchased from Beijing Pulilai Gene Technology Co., Ltd., Beijing, China.

2.8. Real-time PCR

A tissue block was ground in liquid nitrogen and total RNA was isolated in 1 mL Trizol according to per manufacturer’s instructions. Total extracted RNA was

reverse transcribed to cDNA using reverse transcription kit (Kangweishiji, Beijing, China) following the manufacturer's instructions. The cDNA products were amplified by an RT-PCR module and normalized based on the amount of beta actin cDNA. The annealing temperature of OPG, RANKL, and β-actin was 60 ℃. The upstream and downstream primers are shown in Table 1.

Table 1 Primers used in this study

Gene	Primer sequences
OPG	Forward:CGTGAAGAAGGAACTAGCATCTC
	Reverse: ACTGCAAGCAGTAATAAGGGAAA
RANKL	Forward: ACTTTGCGGTACAGGGTCAG
	Reverse: GGCCACGCCTCTTAGTAGTC
beta actin	Forward: TTGTCCCCCAACTTGAGATGTA
	Reverse: GCACTTTTATTGAACTGGTCTCGT

2.9. Statistical analysis

Statistical analyses were performed by using SPSS 20.0 software (IBM, Chicago, IL, USA). Data were represented by mean ± standard deviation ($\bar{x} \pm s$). The comparison among experimental groups was used for one-way analysis of variance, while the multiple comparisons for least significant difference method. Differences were considered statistically significant if $P < 0.05$ and extremely significant if $P < 0.01$.

3. RESULTS

3.1. Acupotomy reduced the Lequesne index score

The behavioral score in the model group was significantly higher than what in the control group ($P < 0.01$). There was no statistical difference in the Lequesne score of each model group before intervention ($P > 0.05$). After immobilizing the hind limbs for 9 weeks, the degree of Gait changes in KOA rabbits was generally found from moderate to severe (2-3 points). After treatment, the scores of the acupotomy ($P < 0.01$) and EA ($P < 0.01$) groups were significantly lower than those of the model group ($P < 0.01$). A lower score indicates better behavior (Table 2).

Table 2 Comparison of the improvement in the Lequesne index in different group ($\bar{x} \pm s$)

Group	*n*	Before treatment	After treatment
Control	6	0.00±0.00	0.0±0.00
Model	6	7.00±0.89[a]	6.83±0.75[a]
Acupotomy	6	7.33±0.82[a]	4.57±0.78[ab]
EA	6	7.33±0.82[a]	4.57±0.78[ab]

Notes: control group: without any treatments and model establishment; model group: treated without acupotomy or electroacupuncture but joined model establishment; Apo (acupotomy group: treated only with acupotomy and joined model establishment; EA (electroacupuncture group): treated only with electroacupuncture and joined model establishment. Compared with the control group, [a]$P < 0.01$; compared with the model group, [b]$P < 0.01$.

3.2. Acupotomy attenuated cartilage degeneration

Rabbits in the control group exhibited clearly distinguished cartilage layers and smooth surface. Chondrocytes are arranged in an orderly and normal shape. The cartilage in KOA group presented cartilage surface abrasion and large defects and chondrocytes appear necrosis and the nucleus shrinks. As the number of normal cells decreased, the number of hypertrophic chondrocytes increased. In addition, the arrangement of cells was disordered and staining of cartilage matrix was heterogeneous. Both acupotomy and EA groups showed a continuously smoother surface and increase of normal chondrocytes, as well as the size and number of hypertrophic chondrocytes decreased. But in EA group, calcified cartilage layer vascular proliferation was evident (Figure 1). Moreover, Mankin scoring suggested that cartilage destruction was more severe in the model group（9.67 ± 1.21 *vs* 0.00 ± 0.00, $P = 0.000 < 0.01$） than what in the control group. In comparison with model group, the Mankin scores in both the acupotomy and EA groups were significantly lower (5.16 ± 1.16, $P = 0.000 < 0.01$ for acupotomy; 7.17 ± 0.75, $P = 0.007 < 0.01$ for EA). Furthermore, we observed a significantly decrease ($P = 0.0409 < 0.05$) in the acupotomy compared with the EA group (Figure 1A). All the results reflect that the cartilage degeneration has been improved after treatment with EA or acupotomy.

Quantitative analysis of the thickness of total articular cartilage (TAC) and the ratio of calcified cartilage to the total articular cartilage (ACC/TAC) by microscopy under 40 × magnification reflected indirectly the degree of cartilage degeneration. The TAC in the model group decreased significantly, and ACC/TAC increased significantly compared to what in the control group (153 ± 64 *vs* 343 ± 66, $P = 0.0005 < 0.01$), while the TAC increased and the ratio of ACC/TAC decreased in the acupotomy and EA groups compared to model group (304 ± 72, $P = 0.0057 < 0.01$ for acupotomy; 278 ± 63, $P = 0.0282 < 0.05$ for EA). Moreover, TAC had a rising tendency in the acupotomy group compared with the EA group ($P > 0.05$). The results showed that both acupotomy and EA alleviated the degeneration of cartilage in KOA rabbits, and more benefits were obtained under acupotomy treatment (Figure 1B, 1C).

3.3. Acupotomy improves the microstructure of subchondral bone

To evaluate the changes of subchondral bone, this study has measured and calculated the thickness of SBP and the ratio of trabecular bone area to total tissue area (BV/TV). The SBP in the model group was markedly higher than what in the control group (341.86 ± 72.70 *vs* 141.13 ± 28.51, $P = 0.0000 < 0.01$), while SBP in the acupotomy and EA groups decreased remarkably compared to what in the model group (196.45 ± 39.33, $P = 0.0002 < 0.01$ for acupotomy; 267.30 ± 25.33, $P = 0.0005 < 0.01$ for EA). Moreover, distinct differences in SBP were observed between the acupotomy and EA groups (196.45 ± 39.33 *vs* 267.30 ± 25.33, $P = 0.0055 < 0.05$) (Figure 2A). As shown in Figure 2B, the level BV/TV was increased in model group compared with the

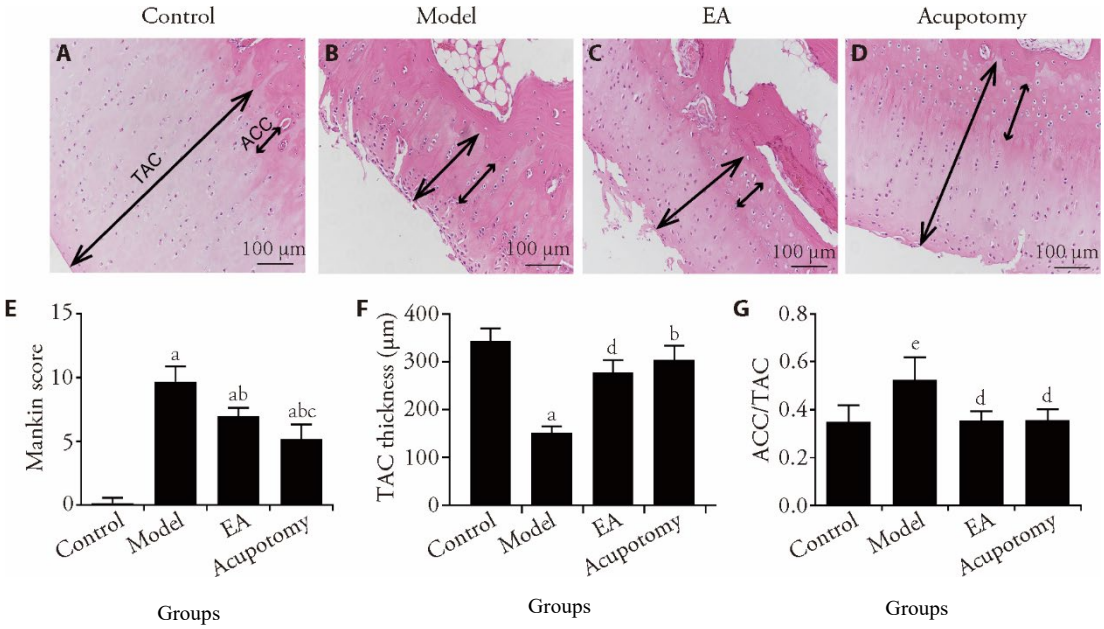

Figure 1 Representative images from the hematoxylin and eosin-stained sections of the Cartilage from various groups
A-D: hematoxylin and eosin-staining (×100); A: control group; B: model group; C: EA group; D: acupotomy group; E: Mankin score of the control, model, EA and acupotomy groups. F, G: quantitative analysis for TAC thickness and the ratio of ACC/TAC. Control group: without any treatments and model establishment; model group: treated without acupotomy or electroacupuncture but joined model establishment; Apo (acupotomy group: treated only with acupotomy and joined model establishment; EA (electroacupuncture group): treated only with electroacupuncture and joined model establishment. Data represents mean ± standard deviation (n = 6). Compared with the control group, $^{a}P < 0.01$, $^{e}P < 0.05$; compared with the model group, $^{b}P < 0.01$, $^{d}P < 0.05$; compared with the EA group, $^{c}P < 0.05$. Hematoxylin-eosin staining cartilage calcified cartilage (ACC) and total articular cartilage (TAC) thickness are marked by double-headed arrows.

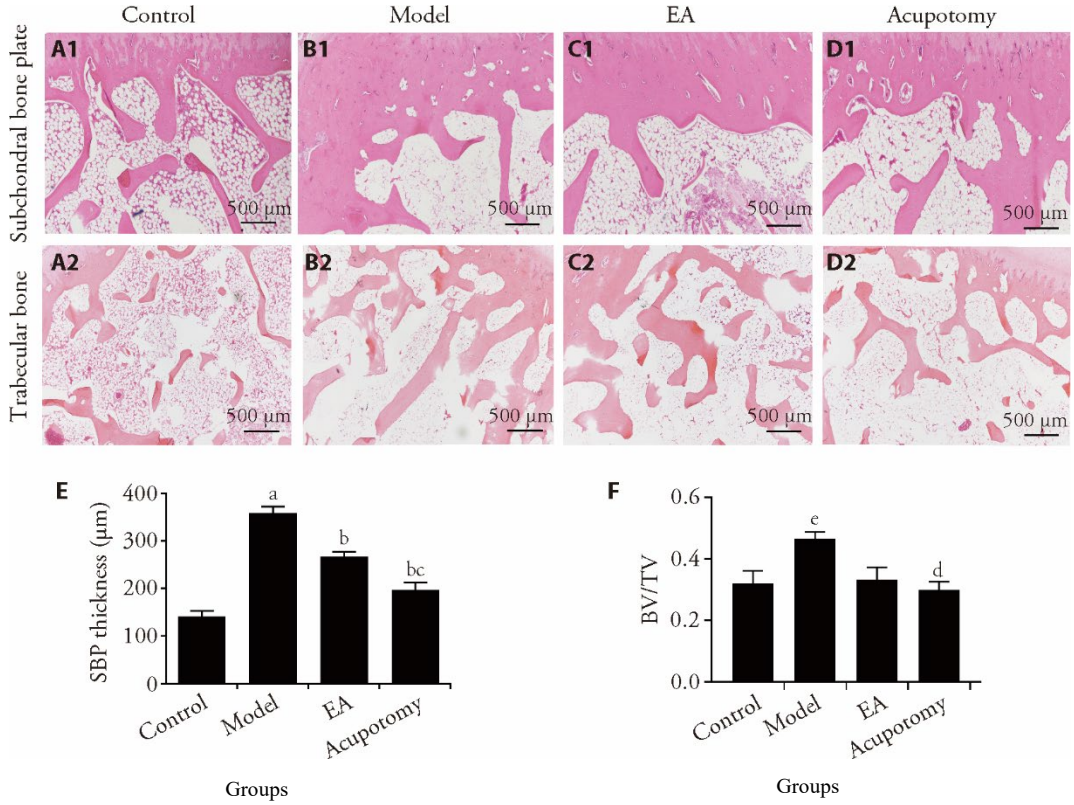

Figure 2 Histomorphometric analysis of subchondral bone
A1-D1: subchondral bone plate (HE staining, × 40); A2-D2: trabecular bone (HE staining, ×40); A1, A2: control group; B1, B2: model group; C1, C2: EA group; D1, D2: acupotomy group. E and F: bone volume/tissue volume (BV/TV) and SBP thickness. Control group: without any treatments and model establishment; model group: treated without acupotomy or electroacupuncture but joined model establishment; Apo (acupotomy group: treated only with acupotomy and joined model establishment; EA (electroacupuncture group): treated only with electroacupuncture and joined model establishment. Data represents mean ± standard deviation (n = 6). Compared with the control group, $^{a}P < 0.01$, $^{e}P < 0.05$; compared with the model group, $^{b}P < 0.01$, $^{d}P < 0.05$; compared with the EA group, $^{c}P < 0.05$.

control group（0.32 ± 0.10 *vs* 0.47 ± 0.05, $P = 0.0253 < 0.05$) and decreased in acupotomy group compared with the model group (0.36 ± 0.11 *vs* 0.47 ± 0.05, $P = 0.0101 < 0.05$). Furthermore, no differences in BV/TV were

observed between the EA and model groups ($P > 0.05$).
A scanning electron microscopy was used to observe the morphology of subchondral bone collagen. Normal collagen fibers were arranged in bundles and crisscrossed regularly. The fiber bundles were uniform in thickness and crossed into a grid. The grid holes were uniform in size and evenly distributed. The collagen fiber bundles in the model group were of various thicknesses, inconsistent shape directions and clusters. The mesh pores formed by the intersection of collagen bundles were of various sizes and distorted shapes. The acupotomy group exhibited regular arrangement of the fiber bundles with clear structure compared with the EA group. Some broken collagen fibers could also be seen in the EA group (Figure 3).

3.4. Acupotomy down-regulated OPG/RANKL ratio

OPG/RANKL/RANK signaling pathway is important in the regulation of bone remodeling. Whether the two kinds of therapies have affected the subchondral bone formation by regulating the expression of OPG/RANKL/RANK was investigated in this study.
Real-time PCR analysis had revealed that the expression of mRNA in OPG was significantly increased ($P < 0.01$) in the model group compared with what in the control group, while it was increased ($P < 0.01$) in the acupotomy group. There was a tendency for the EA group to show a decreasing trend compared with the model group, but there was no statistical significance between them (Figure 4B). Although the expression of mRNA in RANKL in the model group was higher than the control group ($P < 0.05$), the difference between all treated and model groups did not reach statistical significance (Figure 4C).
WB was used to measure the OPG and RANKL protein levels yielded similar results (Figure 4A). The protein expression of OPG was increased ($P < 0.01$) in the model group compared with what in the control group. The OPG level in acupotomy and EA groups were both significantly decreased ($P < 0.01$; $P < 0.05$) than what in the model group (Figure 4E). The results above were further confirmed by immunohistochemical staining (Figure 5A). There was no significant difference found in RANKL level in any group whether using WB or Immunohistochemistry staining (Figure 4F, 5B).
Since OPG and RANKL are both secreted by bone cells, the ratio of the two could better reflect the balance between bone resorption and formation. Therefore, the ratio of OPG/RANKL in different experimental groups was further analyzed in this study. The mRNA and protein ratio of OPG/RANKL exhibited similar results. The model groups showed significantly higher ratio ($P < 0.05$) respectively than what in the control group. The ratio in acupotomy group was significantly reduced compared to the model group ($P < 0.05$). The results suggest that acupotomy may have an indirect effect in regulating osteoclastogenesis via osteoblasts through the OPG/RANKL pathway (Figure 4D, 4G, 5C).

4. DISCUSSION

It was found in this study that the way of model establishment that the rabbits' left hind limbs were immobilized had induced cartilage degeneration and aberrant subchondral bone formation. The knees were immobilized for 9 weeks to establish KOA model on rabbits. This study suggested that acupotomy and EA intervention significantly reduced Lequesne score and improved the knee function. In addition, a correlative approach using light and electron microscopy revealed the promotive effects of acupotomy and EA on the formation of cartilage. It was also observed in this

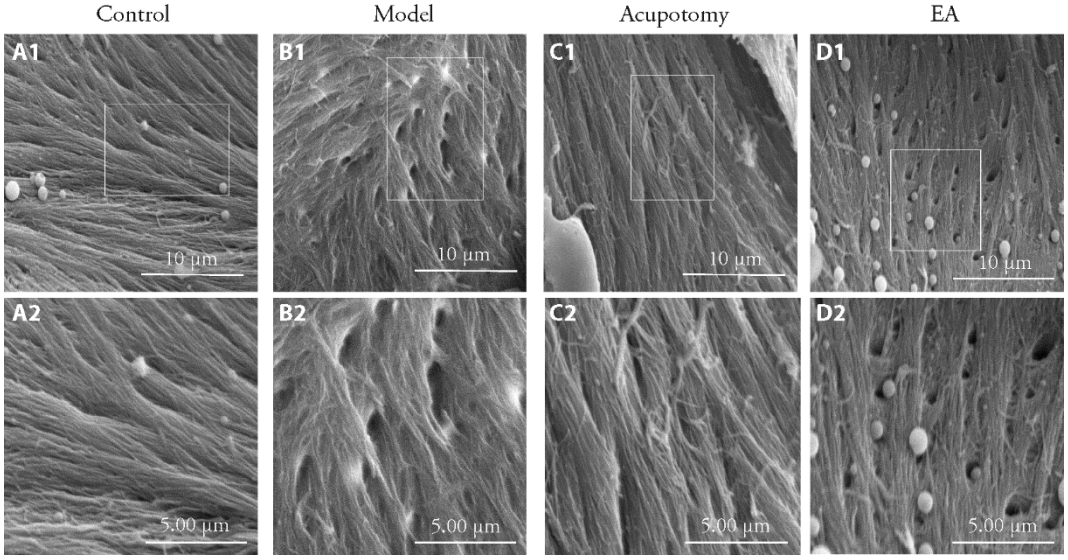

Figure 3 Subchondral bone collagen fiber ultrastructure by scanning electron microscopy in different groups (magnification: ×5000, ×10000)
A1-D1: trabecular bone collagen fiber (magnification: ×5000); A2-D2: trabecular bone collagen fiber (magnification: ×10000); A1, A2: control group; B1, B2: model group; C1, C2: acupotomy group; D1, D2: EA group. Control group: without any treatments and model establishment; model group: treated without acupotomy or electroacupuncture but joined model establishment; Apo (acupotomy group: treated only with acupotomy and joined model establishment; EA (electroacupuncture group): treated only with electroacupuncture and joined model establishment.

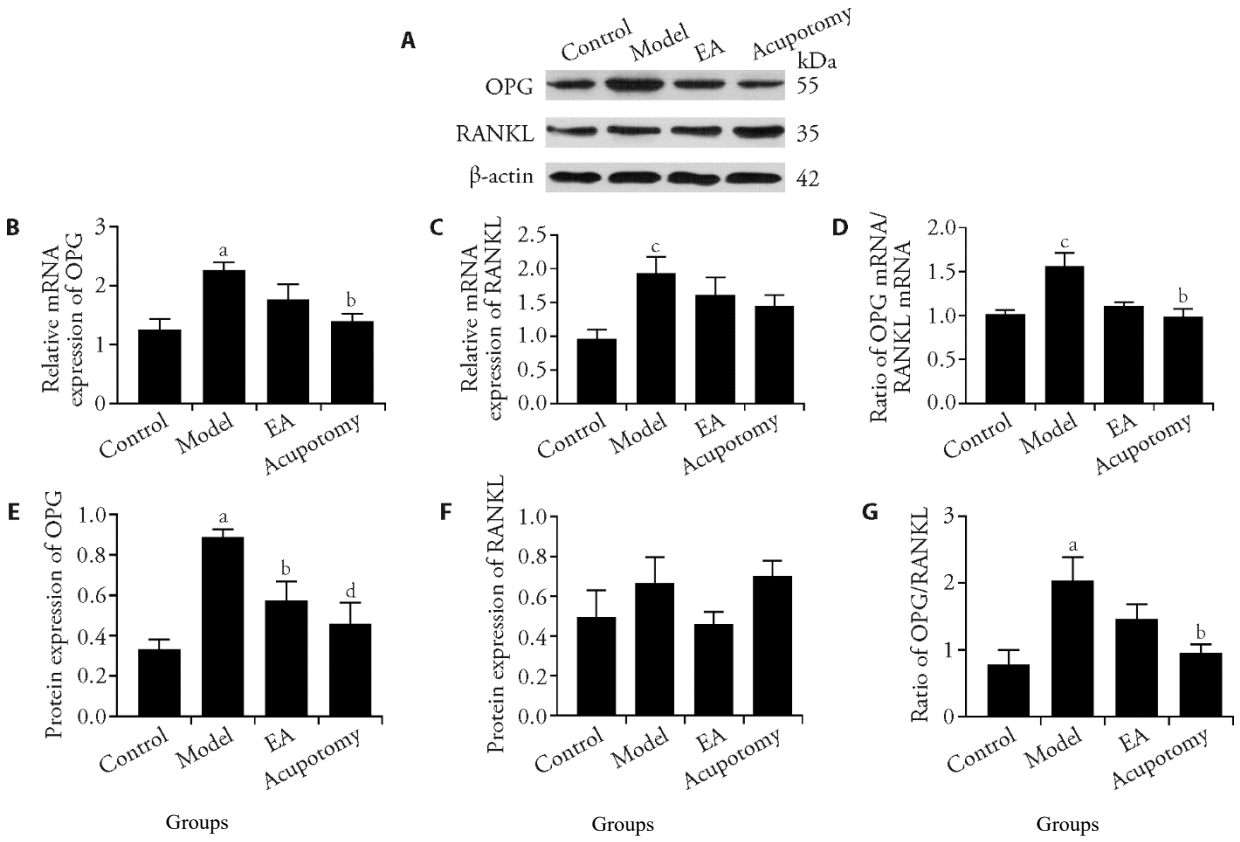

Figure 4 Effects of acupotomy and EA intervention on OPG/RANKL signaling pathway-related genes and proteins expression in subchondral bone

A: protein expression of OPG and RANKL in different groups. **B:** OPG gene expression; **C**: RANKL gene expression; D: ratio of OPG mRNA/RANKL mRNA; E: OPG protein relative abundances; F: RANKL protein relative abundances; **G**: ratio of OPG protein/RANKL protein; Data represents mean ± standard deviation (n = 6). Compared with the control group, $^{a}P < 0.01$, $^{c}P < 0.05$; compared with the model group, $^{d}P < 0.01$, $^{b}P < 0.05$.

research that the expression of OPG protein and thickening of the subchondral bone plate were decreased by acupotomy or EA therapy and acupotomy was more effective at inhibiting aberrant formation of subchondral bone than EA. This difference may result from differences in the regulation of OPG/RANKL ratio.

Numerous spontaneous and induced animal models have been developed to study pathophysiological features and pathogenesis of OA. However, due to the heterogeneity of the disease, there is no single animal model that reflects the progression of OA in humans. Thus model selection is based on the experiment, the funding and the modeling mechanism. Compare to the big animal models, such as dogs, goats and horses, smaller ones such as mice, rats, guinea pigs and rabbits cost less and could be operated more easily.[19] Considering the size of the edge of acupotome which would cause serious damage to small animals, adult rabbits are comparatively suitalble to be the model animal. The KOA models could be induced chemically, surgically and mechanically. Nonetheless, the chemical drug-induced model would cause extensive lesions, and the mechanism of human OA is different with it. In addition, it is difficult to restore the biomechanical balance of joint instability caused by surgical methods. Moreover, the two-way induced models are not suitable for studying the pathogenesis of naturally occurred primary degenerative osteoarthritis.[20] Thus the way of long-term knee immobilization was applied in this study to establish the KOA model. Knee joint immobilization leads to continuous contraction of the muscles and joint sacs, which would result in cartilage destruction and weakens the quadriceps muscle and induce KOA.[17] Compared with other experimental KOA models, the way to establish the model in this study better simulated the natural process of human KOA.[21] and is more suitable for studying the effect of acupomy therapy based on releasing tendon adhesion and remitting tension.

In this study, KOA rabbits presented clear signs of limping, joints stiffness and decreased range of knee motion. The histological analysis of cartilage showed that the thickness of total cartilage decreased whereas calcified cartilage layer thickened. All these changes indicated that the cartilage is degenerative and the method of knee joint immobilization could successfully replicate the OA model. Furthermore, HE staining showed thickening of the subchondral bone plate and immunohistochemistry staining showed active osteoblasts gather around bone trabeculae. These pathological changes were all similar to what in the middle and late stages of human KOA.[22,23] Therefore, the rabbit left hind limb immobilization for 9 weeks could mimics the pathological changes in human KOA.

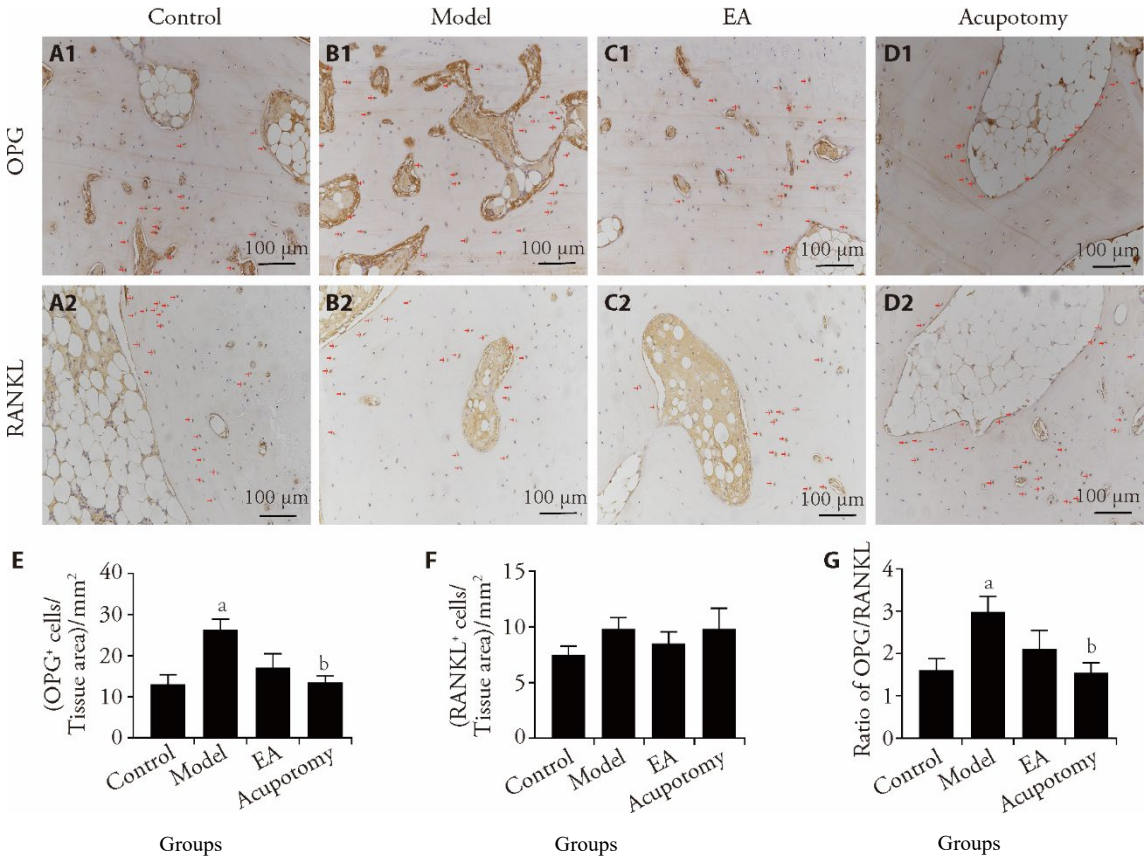

Figure 5 Immunohistochemical detection of RANKL and OPG in rabbits subchondral bone of different groups, and staining densities were quantified by IPP analysis.
A1-D1: OPG; A2-D2: RANKL; A1, A2: control group; B1, B2: model group; C1, C2: EA group; D1, D2: acupotomy group. E, F: The mean ± SE staining density for RANKL (E) or OPG (F) protein expression. G: The mean RANKL/OPG ratio for protein expression. Data represents mean ± standard deviation (n = 6). Compared with the control group, $^{a}P < 0.05$; compared with the model group, $^{b}P < 0.05$. The red arrows represent cells positive for OPG and RANKL. OPG: Osteoprotegerin; RANKL: receptor activator of nuclear factor-κB ligand.

Under normal physiological loading, the elastic modulus of subchondral bone is lower than that of articular cartilage, while the quantity is relatively large, which is conducive to providing mechanical support for cartilage during shocks to protect articular cartilage from excessive stress damage. However, abnormal stress and strain in knee joint could result in aberrant subchondral bone remodeling[24] According to Wolff's Law, the internal architecture of bone develops according to the magnitude and direction of the loading force.[25] In order to accommodate the increased mechanical forces during intermediate or advanced OA, the subchondral bone plates thickened and sclerosis would occur, and the density and volume of bone would be increased, which had been demonstrated in humans and in vivo animal studies.[26,27] However, during this period, the degree of mineralization in subchondral bone was inadequate and the material stiffness was reduced, which might aggravate cartilage degeneration.[28]

It is believed that excessive mechanical stress is an important factor in OA pathogenesis, [29, 30] and the pathological changes of OA include articular cartilage degeneration, subchondral bone remodeling, angiogenesis, higher bone formation and sclerosis.[31, 32] However, there is still no specific cure for KOA. Although both the most up-to-date guidelines of the European Society for Clinical and Economic Aspects of Osteoporosis and Osteoarthritis (ESCEO) and Osteoarthritis Society International (OARSI) recommend NSAIDs as the first-line pharmacological treatment for KOA, [33, 34] there are still certain limitations to the clinical application of NSAIDs. The way to ameliorate cartilage degeneration is still critical to alleviating OA development and progress. Biomechanical therapy is a novel treatment option for KOA by re-balancing the knee loading. Tendons often transfer tremendous force from muscles to bones to stabilize joint movement. The region where tendons and ligaments attach to bone is a site of stress concentration. This tissue overloading lead to inflammation and pain.[35] Since knee flexion and extension are controlled by the biceps femoris and quadriceps muscles, and the anserina bursa is the most common site for pain and inflammation with knee osteoarthritis, [36] we choose the endpoint of biceps femorisas, quadriceps femoris and the anserina bursa as stimulation points.

The acupoints Neixiyan (EX-LE4), Waixiyan (ST35), and Ququan (LR8), Weiyang (BL39) which are close to biceps femoris were chosen as EA treatment points. Neixiyan (EX-LE4) and Waixiyan (EX-LE5) are located

in the inner and outer depressions of the patellar ligament. The needles can penetrate directly into the knee joint cavity and the EA electrode circuit could be established between these two acupoints. Stimulating the acupoints around the joint reduce the pressure in the knee joint cavity, promote blood circulation, improve tissue nutrition, and relieves muscle tension, which improves the biomechanical balance of the knee.[37] In addition, Weiyang (BL39) is located on the inner edge of the biceps femoris tendon, and Ququan(LR8) is located on the posterior edge of the medial femur. Studies have shown that EA could relieve muscle cramps, increase muscle strength and improve mobility joint range of motion through the stimulation of acupoints.38 There are the symptoms of muscle spasm at the back of the knee joint in KOA, and EA treatment on Weiyang (BL39) and Ququan (LR8) helps to alleviate muscle spasm and enhance muscle strength.[38] Acupotomy is a medical device which penetrates into the skin like a needle and cuts and separates the tissues like a mini-knife.[39] The tip of acupotomy separates the adhesion or contracture of the soft tissue to restore the mechanical balance of the joint.[40] While generally, the tip of needle applied in EA is smaller than acupotomy, EA is less effective in releasing soft tissue adhesion or reducing the pressure of the joint cavity than acupotomy.[41]

The coordination of knee extensors and flexors helps to evenly distribute the load and avoid stress concentration on the cartilage surface.[42] The previous studies have shown that acupotomy intervention improved the mechanical properties of ligaments, tendons and muscles by releasing the tendons around the knee joint.[43-45] This effect removed the abnomal mechanical stress distribution on the cartilage, thereby alleviating its degradation.[15,16] The benign biomechanical effect of acupotomy has beenwas confirmed. Considering the role of subchondral bone in KOA, the role of acupotomy on subchondral bone should be further explored, for example, whether the benign mechanical effect of the acupotomy improves subchondral bone remodeling, and whether the benign mechanical effect reduces the abnormal bone formation through the OPG/RANKL/ RANK mechanically sensitive pathway.

Cartilage damage is the golden standard for the indexes evaluating KOA, and Mankin score is the most commonly accepted and widely used system for evaluating the cartilage damage. In the current animal model of this study, the HE staining showed cartilage destruction in KOA model rabbits, including superficial fibrillation, surface cracks and ulcers, and vertical micro-fractures that extended into deeper cartilage layers. After acupotomy or EA treatment, the aforementioned pathological alterations were observed to be alleviated. In addition, acupotomy intervention may reduce Mankin score to a greater extent and have a better tendency to recover TAC thickness than EA. The results are consistent with our previous studies, which indicate that the mechanical effects of acupotomy provides significantly better cartilage protection than EA.[46]

The mechanical overloading would result in ultrastructural damage of the subchondral bone, which would in turn destroy the integrity of the subchondral bone, increase the load of covering cartilage, and would ultimately lead to cartilage damage and degradation.[47] Studies confirmed that proper knee loading reduced the abnormal bone mass at advanced stage of OA.[48] Thus, the inhibition of abnormal subchondral bone formation may improve subchondral bone microstructure and alleviate cartilage degeneration, which would be beneficial to retard the process of OA.[49,50] Compared with the model group, both acupotomy and EA reduced the thickness of subchondral bone plate and bone volume fraction, but the inhibitory effect of acupotomy on abnormal formation of subchondral bone was better than what in EA group. The results indicate that the effect of acupotomy in correcting the abnormal mechanical load of the joint and inhibiting the remodeling of the subchondral bone of KOA is significantly better than that of EA.

It was further examined in this study the morphology changes in subchondral bone collagen with electron microscope. The arrangement of .bone collagen is vital to its mechanical behavior, and its mechanical loading changed the orientation of the collagen fibril.[51, 52] From the KOA patients, the ultrastructure of the collagen fibers in the subchondral bone were seen to be poorly aligned.[53] These abnormal arrangement of collagen were also observed in KOA rabbits in this study. Furthermore, bundles of well-oriented bone fibrils were also displayed in acupotomy group. These results further illustrate that the benign mechanical effects of acupotomy could improve the subchondral bone structure of OA.

The discovery of the OPG/RANKL/RANK pathway is a major advance in understanding the molecular mechanism of bone remodeling. Studies have confirmed that the OPG/RANKL/RANK pathway was proved to be mechanically sensitive. In addition to the individual effects of RANKL and OPG, the ratio of OPG/RANKL was a determinant of bone formation and resorption.[54] Studies have revealed that appropriate stress stimulation up-regulated the expression level of RANKL and other genes in KOA subchondral osteoblasts, whilst down regulating the gene or protein expression level of OPG.[55] Thus, benign mechanical stress could inhibit the abnormal subchondral bone formation in KOA and promote the repair of subchondral bone after injury. It was shown in this study that in immobilization induced KOA model rabbits, the expression and secretion of OPG protein were increased, whereas RANKL protein expression just showed a downward trend. Consequently, increased OPG to RANKL ratios favour bone turnover and greater bone formation. Subsequent to 3 weeks of treatment, acupotomy down-regulated OPG mRNA and protein expression, and leaded to statistically significantly decreased OPG/RANKL ratio. Despite EA has a down-regulated OPG protein expression, the OPG/RANKL ratio showed no significant decrease when

compared with the model group. The above results indicate that acupotomy have a stronger inhibitory effect on aberrant formation of subchondral bone compared with EA. Expression of OPG and RANKL is affected by mechanical strength, frequency and stimulus duration. This may be attribute to the different mechanical stimulation of EA and acupotomy.

However, we found no significant difference in RANKL expression among different groups. The researches of RANKL and OPG expression in various cells under different mechanical conditions have been reported. In the sclerotic areas of human OA subchondral bone, compression decreased the expression of OPG but reduced the expression of RANKL.[55] Another research showed that compressive force or mechanical vibration or compressive force combined with mechanical vibration neither enhanced nor inhibited the expression of RANKL and OPG in osteoblasts.[56] Moreover, a tensile strain upregulated OPG expression and downregulated RANKL expression.[57] These researches demonstrated that the increase or decrease of RANKL by mechanical stimulation may be caused by different type of loading. Unlike *in vitro* experiments, the mechanical stimulus might be complex *in vivo*, for which we could not monitor the type loading of acupotomy. Our limited data do not suggest RANKL mRNA and protein statistically significant increased after treatment of acupotomy or EA, which may be attribute to the mechanical effect of acupotomy that it is more inclined to control OPG but has little effect on the expression of RANKL.

The major limitation of this study is the absence of positive drug control group. We have thought about the possibility of setting bisphosphonate, the bone metabolism regulator as the positive drug group, but its effect on osteoarthritis is still controversial.[58] The pathogenesis of KOA is complex and involves multiple factors, such as inflammation and metabolic factors, there is currently no effective biomechanical treatment for OA.[59] As a non-surgical-drug therapy, EA is currently well-recognized as an effective treatment for KOA, although its mechanism is still being explored. Moreover, the biomechanical therapy was mainly applied in this study, and the subchondral bone was as the target of treatment. The acupoints of EA treatment for KOA were similar with what in acupotomy. Therefore, the EA group was set as the control group for acupotomy. Further studies should be made when there would be better biomechanical treatments in the future. Another limitation of this study is the lack of sham EA group, which is lack of strong evidence for the specificity of the mechanism of acupoint treatment of KOA. Research has shown that true EA could improve muscle mechanical properties than the sham EA,[60] however, the specific mechanisms of acupoint in treatment of KOA still need in-depth research. These improvements will be accomplished in our forthcoming work.

In conclusion, this study has shown that acupotomy inhibit subchondral bone abnormal formation during the process of KOA development, which may due to the down-regulation of OPG/RANKL. The effect of acupotomy is slightly greater than that of EA therapy. Acupotomy is an appropriate complementary and alternative therapy to alleviate cartilage degeneration and inhibits aberrant formation of subchondral bone of knee osteoarthritis. Therefore, acupotomy might provide a new promising strategy as a therapeutic approach for patients with KOA.

5. REFERENCES

1. Vos T, Flaxman AD, Naghavi M, et al. Years lived with disability (YLDs) for 1160 sequelae of 289 diseases and injuries 1990-2010: a systematic analysis for the Global Burden of Disease Study 2010. Lancet 2012; 380: 2163-96.
2. Lane NE, Shidara K, Wise BL. Osteoarthritis year in review 2016: clinical. Osteoarthritis Cartilage 2017; 25: 209-15.
3. Nelson AE, Allen KD, Golightly YM, Goode AP, Jordan JM. A systematic review of recommendations and guidelines for the management of osteoarthritis: the chronic osteoarthritis management initiative of the U.S. bone and joint initiative. Semin Arthritis Rheum 2014; 43: 701-12.
4. Hugle T, Geurts J. What drives osteoarthritis-synovial versus subchondral bone pathology. Rheumatology (Oxford) 2017; 56: 1461-71.
5. Iijima H, Aoyama T, Ito A, et al. Immature articular cartilage and subchondral bone covered by menisci are potentially susceptive to mechanical load. BMC Musculoskelet Disord 2014; 15: 101.
6. Chen X, Wang ZQ, Duan N, Zhu GY, Schwarz EM, Xie C. Osteoblast-osteoclast interactions. Connect Tissue Res 2018; 59: 99-107.
7. Zhen G, Wen C, Jia XF, et al. Inhibition of TGF-beta signaling in mesenchymal stem cells of subchondral bone attenuates osteoarthritis. Nat Med 2013; 19: 704-12.
8. Holzer LA, Kraiger M, Talakic E, et al. Microstructural analysis of subchondral bone in knee osteoarthritis. Osteoporos Int 2020; 31: 2037-45.
9. Findlay DM, Atkins GJ. Osteoblast-chondrocyte interactions in osteoarthritis. Curr Osteoporos Rep 2014; 12: 127-34.
10. Bellido M, Lugo L, Roman-Blas JA, et al. Subchondral bone microstructural damage by increased remodelling aggravates experimental osteoarthritis preceded by osteoporosis. Arthritis Res Ther 2010; 12: R152.
11. Schaffler MB, Kennedy OD. Osteocyte signaling in bone. Curr Osteoporos Rep 2012; 10: 118-25.
12. Zhou XC, Cao H, Yuan Y, Wu W. Biochemical Signals Mediate the Crosstalk between Cartilage and Bone in Osteoarthritis. Biomed Res Int 2020; 2020: 5720360.
13. Felson DT. Osteoarthritis as a disease of mechanics. Osteoarthritis Cartilage 2013; 21: 10-5.
14. Lin M, Li X, Liang WN, et al. Needle-knife therapy improves the clinical symptoms of knee osteoarthritis by inhibiting the expression of inflammatory cytokines. Exp Ther Med 2014; 7: 835-42.
15. Ma SN, Xie ZG, Guo Y, et al. Effect of acupotomy on FAK-PI3K signaling pathways in KOA rabbit articular cartilages. Evid Based Complement Alternat Med 2017; 2017: 4535326.
16. Liang CX, Guo Y, Tao L, et al. Effects of acupotomy intervention on regional pathological changes and expression of cartilage-mechanics related proteins in rabbits with knee osteoarthritis. Zhen Ci Yan Jiu 2015; 40: 119-24, 140.
17. Langenskiold A, Michelsson JE, Videman T. Osteoarthritis of the knee in the rabbit produced by immobilization. Attempts to achieve a reproducible model for studies on pathogenesis and therapy. Acta Orthop Scand 1979; 50: 1-14.
18. Nagira K, Ikuta Y, Shinohara M, et al. Histological scoring system for subchondral bone changes in murine models of joint aging and osteoarthritis. Sci Rep 2020; 10: 10077.
19. Mitchell RE, Huitema LF, Skinner RE, et al. New tools for studying osteoarthritis genetics in zebrafish. Osteoarthritis Cartilage 2013; 21: 269-78.

20. Samvelyan HJ, Hughes D, Stevens C, Staines KA. Models of osteoarthritis: relevance and new insights. Calcif Tissue Int 2021; 109:243-56.
21. Li W, Lin JJ, Wang ZW, et al. Bevacizumab tested for treatment of knee osteoarthritis *via* inhibition of synovial vascular hyperplasia in rabbits. J Orthop Translat 2019; 19: 38-46.
22. Matsui H, Shimizu M, Tsuji H. Cartilage and subchondral bone interaction in osteoarthrosis of human knee joint: a histological and histomorphometric study. Microsc Res Tech 1997; 37: 333-42.
23. Finnila M, Thevenot J, Aho OM, et al. Association between subchondral bone structure and osteoarthritis histopathological grade. J Orthop Res 2017; 35: 785-92.
24. Boyd SK, Muller R, Zernicke RF. Mechanical and architectural bone adaptation in early stage experimental osteoarthritis. J Bone Miner Res 2002; 17: 687-94.
25. Frost HM. From Wolff's law to the Utah paradigm: insights about bone physiology and its clinical applications. Anat Rec 2001; 262: 398-419.
26. Matsui H, Shimizu M, Tsuji H. Cartilage and subchondral bone interaction in osteoarthrosis of human knee joint: a histological and histomorphometric study. Microsc Res Tech 1997; 37: 333-42.
27. Nakasa T, Ishikawa M, Takada T, Miyaki S, Ochi M. Attenuation of cartilage degeneration by calcitonin gene-related paptide receptor antagonist *via* inhibition of subchondral bone sclerosis in osteoarthritis mice. J Orthop Res 2016; 34: 1177-84.
28. Zhu XB, Chan YT, Yung PSH, Tuan RS, Jiang Y. Subchondral bone remodeling: a therapeutic target for osteoarthritis. Front Cell Dev Biol 2020; 8: 607764.
29. Xu B, Xing RL, Huang ZQ, et al. Excessive mechanical stress induces chondrocyte apoptosis through TRPV4 in an anterior cruciate ligament-transected rat osteoarthritis model. Life Sci 2019; 228: 158-66.
30. He ZN, Nie PF, Lu JL, et al. Less mechanical loading attenuates osteoarthritis by reducing cartilage degeneration, subchondral bone remodelling, secondary inflammation, and activation of NLRP3 inflammasome. Bone Joint Res 2020; 9: 731-41.
31. Wu L, Guo HH, Sun KN, Zhao X, Ma T, Jin CH. Sclerostin expression in the subchondral bone of patients with knee osteoarthritis. Int J Mol Med 2016; 38: 1395-402.
32. Cui Z, Crane J, Xie H, et al. Halofuginone attenuates osteoarthritis by inhibition of TGF-beta activity and H-type vessel formation in subchondral bone. Ann Rheum Dis 2016; 75: 1714-21.
33. Bannuru RR, Osani MC, Vaysbrot EE, et al. OARSI guidelines for the non-surgical management of knee, hip, and polyarticular osteoarthritis. Osteoarthritis Cartilage 2019; 27: 1578-89.
34. Arden NK, Perry TA, Bannuru RR, et al. Non-surgical management of knee osteoarthritis: comparison of ESCEO and OARSI 2019 guidelines. Nat Rev Rheumatol 2021; 17: 59-66.
35. Greif DN, Emerson CP, Jose J, Toumi H, Best TM. Enthesopathy-an underappreciated role in osteoarthritis? Curr Sports Med Rep 2020; 19: 495-7.
36. Resorlu M, Doner D, Karatag O, Toprak CA. The Relationship between chondromalacia patella, medial meniscal tear and medial periarticular bursitis in patients with osteoarthritis. Radiol Oncol 2017; 51: 401-6.
37. Zhong WQ, Lao JX, Li SC, et al. Observation on the difference of curative effect between Neixiyan and Waixiyan on degenerative knee osteoarthritis. Guang Ming Zhong Yi 2011; 26: 108-9.
38. Que Q H, He F, Wang J, et al. Application of five points behind the knee combined with electroacupuncture in the treatment of early knee osteoarthritis. Rehabilitation Medicine 2014; 24: 55-6.
39. Zhang TM, Zhang Q, Zeng CX, et al. The tool and effect principle of acupotomology. Zhong Guo Yi Yao Dao Bao 2016; 13: 163-6.
40. Liu BZ. Study on the etiology and pathology of chronic soft tissue injury and the mechanism of acupotomy. Zhong Guo Zhong Yi Yao Xian Dai Yuan Chen Jiao Yu 2012; 10: 58-60.
41. Lin WC, Liu CY, Tang CL, Hsu CH. Acupuncture and small needle scalpel therapy in the treatment of calcifying tendonitis of the gluteus medius: a case report. Acupunct Med 2012; 30.
42. Mills K, Hunt MA, Leigh R, Ferber R. A systematic review and Meta-analysis of lower limb neuromuscular alterations associated with knee osteoarthritis during level walking. Clin Biomech (Bristol, Avon) 2013; 28: 713-24.
43. Fu D E L, Guo CQ, Jin XF, et al. Effect of acupotomy treatment on tensile mechanical properties of medial collateral ligaments in a rabbit model of knee osteoarthritis. Shi Jie Zhong Yi Yao 2014; 9: 912-5.
44. Wang LJ, Shi XW, Zhang W, Wang T, Zhou S, Guo CQ. Effect of needle knife intervention on tensile mechanics of femoral quadriceps tendon in rabbits with knee osteoarthritis. Zhong Guo Gu Shang 2019; 32: 462-8.
45. Hu B, Yu JN, Zhang HF, Liu NG, Guo CQ. Effect of acupotomy intervention on contractility of quadriceps femoris and pathological changes of articular cartilage in KOA rabbits. Zhen Jiu Lin Chuang Za Zhi 2018; 34: 50-4.
46. Gao Y, Wang T, Zhang W, et al. Effect of acupotomy on chondrocyte proliferation and expression of CyclinD1, CDK4 and CDK6 in rabbits with knee osteoarthritis. J Tradit Chin Med Sci 2019; 6: 277-91.
47. Schaffler MB, Kennedy OD. Osteocyte signaling in bone. Curr Osteoporos Rep 2012; 10: 118-25.
48. Zheng WW, Li XL, Liu DQ, et al. Mechanical loading mitigates osteoarthritis symptoms by regulating endoplasmic reticulum stress and autophagy. Faseb J 2019; 33: 4077-88.
49. Zhen G, Wen C, Jia X, et al. Inhibition of TGF-beta signaling in mesenchymal stem cells of subchondral bone attenuates osteoarthritis. Nat Med 2013; 19: 704-12.
50. Lin CX, Liu LL, Zeng C, et al. Activation of mTORC1 in subchondral bone preosteoblasts promotes osteoarthritis by stimulating bone sclerosis and secretion of CXCL12. Bone Res 2019; 7: 5.
51. Yang PF, Nie XT, Zhao DD, et al. Deformation regimes of collagen fibrils in cortical bone revealed by in situ morphology and elastic modulus observations under mechanical loading. J Mech Behav Biomed Mater 2018; 79: 115-21.
52. Garnero P. The role of collagen organization on the properties of bone. Calcif Tissue Int 2015; 97: 229-40.
53. Bailey AJ, Sims TJ, Knott L. Phenotypic expression of osteoblast collagen in osteoarthritic bone: production of type I homotrimer. Int J Biochem Cell Biol 2002; 34: 176-82.
54. Zhang Y, Paul EM, Sathyendra V, et al. Enhanced osteoclastic resorption and responsiveness to mechanical load in gap junction deficient bone. PLoS One 2011; 6: e23516.
55. Sanchez C, Pesesse L, Gabay O, et al. Regulation of subchondral bone osteoblast metabolism by cyclic compression. Arthritis Rheum 2012; 64: 1193-203.
56. Chatmahamongkol C, Pravitharangul A, Suttapreyasri S, Leethanakul C. The effect of compressive force combined with mechanical vibration on human alveolar bone osteoblasts. J Oral Biol Craniofac Res 2019; 9: 81-5.
57. Wu YQ, Zhang P, Dai QG, et al. Osteoclastogenesis accompanying early osteoblastic differentiation of BMSCs promoted by mechanical stretch. Biomed Rep 2013; 1: 474-8.
58. Vaysbrot EE, Osani MC, Musetti MC, McAlindon TE, Bannuru RR. Are bisphosphonates efficacious in knee osteoarthritis? A Meta-analysis of randomized controlled trials. Osteoarthritis Cartilage 2018; 26: 154-64.
59. Martel-Pelletier J, Barr AJ, Cicuttini FM, et al. Osteoarthritis. Nat Rev Dis Primers 2016; 2: 16072.
60. Sun YJ, Wu YC, Zhang FJ, Zhang P, Tang ZY. Effects of electroacupuncture on muscle state and electrophysiological changes in rabbits with lumbar nerve root compression. Chin J Integr Med 2013; 19: 446-52.